

## Measurement of High-Energy Neutrons at ISS by SEDA-AP-FIB

K. KOGA<sup>1</sup>, T. GOKA<sup>1</sup>, H. MATSUMOTO<sup>1</sup>, T. OBARA<sup>1</sup>, O. OKUDAIRA<sup>1</sup>, Y. MURAKI<sup>2,3</sup>, T. YAMAMOTO<sup>3</sup>

<sup>1</sup>*Tsukuba Space Center, JAXA, Tsukuba 305-8505, Japan*

<sup>2</sup>*Solar-Terrestrial Environment Laboratory, Nagoya University, Nagoya 464-8601, Japan*

<sup>3</sup>*Department of Physics, Konan University, Kobe 658-8501, Japan*

*muraki@stelab.nagoya-u.ac.jp, muraki@konan-u.ac.jp*

DOI: 10.7529/ICRC2011/V10/0370

**Abstract:** A new type of solar neutron detector (NEM) was launched by the space shuttle Endeavour on July 16th, 2009 and it began collecting data on August 25th, 2009 at the International Space Station (ISS). In this paper we introduce not only preliminary results obtained by the NEM-FIB detector but also a possible solar neutron detection in association with the M3.7 solar flare on March 7, 2011.

**Keywords:** solar neutrons, particle acceleration at the sun, flares

## 1 Introduction

The Space Environment Data Acquisition equipment - Attached Payload (SEDA-AP) detector was first proposed for the measurement of radiation levels at the International Space Station (ISS) in 1991 [1]. It was designed as one of the detectors onboard the Japan Exposure Module, JEM-ISS. It comprises not only a neutron detector (NEM) but also various other detectors such as charged particle detectors (HIT and SDOM), a plasma detector (PLAM), an atomic oxygen monitor (AOM), electronic device evaluation equipment (EDEE and SEED) and the system even includes a micro-particle capture detector (MPAC). The MPAC and SEED have been returned back to Earth by the astronauts. Technical details can be found on the JAXA Website [<http://kibo.jaxa.jp/en/experiment/ef/seda-ap>]

A new solar neutron detector was launched on July 16th, 2009 by the space shuttle Endeavour, and began operation on the ISS on August 25th, 2009. Although the official mission lifetime has been estimated to be 3 years, given the importance of the measurements, it would be highly desirable to extend this to cover at least one solar cycle of 11 years, if the system continues to operate.

## 2 Scientific Purpose

There are three main scientific goals in this experiment.

(1) Accurate measurements of radiation levels in the environment of the ISS. It had been estimated that astronauts who stay on the ISS for one year receive an equivalent radiation dose of 300 mSy [2] during quiescent solar periods. However, no precise data was available for neutrons,

and measurement of the neutron background at the ISS was thus a high-priority task.

(2) Rapid prediction of the imminent arrival of large numbers of charged particles from the Sun by monitoring neutron levels. Such particles are produced by large solar flares and are transported to the Earth by the interplanetary magnetic field. Since they are trapped in the magnetic field, they arrive at the Earth a few hours later than the light associated with the flare. They are sometimes observed by the ground level detectors and known as Ground Level Enhancements.

It of course depends on the position of the flare on the solar surface and the momentum of charged particles, but according to the observation by GOES satellite, even in the quickest case, these particles lag the light by about 20 minutes [3]. However, since neutrons do not interact with the magnetic field, they arrive at Earth's upper atmosphere earlier than the charged particles. Thus, if a large X-class solar flare is detected by the GOES satellite, and is immediately followed by an increased neutron flux in the vicinity of the ISS, then the arrival of a large number of charged particles can be predicted. This would allow the astronauts working on the ISS to take preventative measures by remaining behind a thick aluminum wall until the charged-particle storm has passed. Thus, this corresponds to space weather forecasting.

(3) The establishment of an acceleration model for charged particles above the solar surface is an important issue in cosmic-ray physics. We wish to know *when* and *how* these particles are accelerated. When they finally arrive at Earth and are detected, important information may be lost concerning the timing of their departure from the Sun. To i-

identify the acceleration mechanism of particles at the Sun, it is necessary to compare the data of neutral particles such as gamma-rays and neutrons with images taken by a soft X-ray telescope.

For such a purpose, it is essential to employ a new type of neutron detector that can measure the energy of neutrons and directions. Until now no such detector has been launched into space, although the ground-based Solar Neutron Telescope (SONTEL) has been operating for a number of years [4-7]. Thus, the NEM-FIB detector installed in the SEDA-AP is the first attempt at meeting the challenge of neutron energy measurement in space.

### 3 Detector design, performance and trigger

In order to achieve the scientific goals listed above, a fine-grated neutron detector (referred to as the FIB detector) has been designed. It consists of a  $16 \times 16$  stack of scintillation bars, each with dimensions of  $3\text{mm} \times 6\text{mm} \times 96\text{mm}$  (length). An optical fiber is coupled to the end of each bar to collect photons produced in the scintillator. These are sent to a 256-channel multi-anode-photomultiplier (Hamamatsu H4140-20). A schematic image of the FIB detector is shown in Fig. 1. It measures the tracks of recoil protons produced by incident neutrons and determines the neutron energy using the range method.

We use the range method to estimate the energy of the neutrons. Neutrons are converted into protons via a charge-exchange process when they collide with the hydrogen target in the plastic scintillator. The momentum of the incoming neutrons is transferred to these protons. In the case of solar neutrons, the direction of the source (the Sun) is known, so we can measure the momentum of incoming solar neutrons. Let us assume the angle between the trajectory of the recoil protons and the incident neutron direction as  $\theta$  (Fig. 1). Then the energy of the incoming neutrons ( $E_n$ ) can be uniquely determined using the equation  $E_n = E_p/(\sin\theta)^2$ , if we assume an n-p scattering process. Here  $E_p$  represents the energy of the recoiled protons. Details of the detector have been published elsewhere [8-9].

We measured the energy resolution of the sensor using the Riken proton beam and obtained a value of  $\Delta E/E = [14/\sqrt{E_p}/100\text{MeV} - 10.3]\%$ . For example, the detector has an energy resolution of 4% at  $E_p = 100$  MeV and 13% at  $E_p = 36$  MeV. The details have been published elsewhere [10].

As shown in Figure 1, the neutron detector has a cubic shape with sides of 10 cm. The maximum measurable momentum is about 120 MeV/c. The sensor is monitored from two directions by two 256-channel multi-anode photomultipliers and the arrival direction of the tracks can be identified. To determine the arrival direction of neutrons, protons must penetrate at least four layers of the scintillating bars, each of which consists of 3-mm-thick plastic bars. This corresponds to 35 MeV as the lowest momentum of protons that can identify the direction.

Discrimination between neutrons and protons is achieved by an anti-coincidence system comprising 6 scintillator plates surrounding the FIB sensor in a cubic arrangement. The effectiveness of the anti-coincidence system in rejecting signals due to charged particles was evaluated using the accelerator beam at Riken. The FM was irradiated with a charged particle beam with an intensity of one million particles/sec and an energy of 160 MeV/n. No neutron detection event was identified by the internal sensor. However, when an aluminum target was placed in front of the module, the sensor immediately began to identify neutron signals. Actually we are taking the neutron data over SAA. The counting rate of the anti-coincidence system at SAA is 60,000 counts/sec (at the maximum) and it works.

Below 15 Hz of the trigger rate, both the range and the direction of the generated protons can be measured. Above this frequency, the system cannot obtain information on proton tracks, and the incident neutron flux is recorded based on the dynode signals alone. The question that arises is when a large solar flare occurs, producing neutrons at the solar surface, will it be possible to measure the tracks of all neutrons? Based on the results of our previous Monte Carlo simulations [10-11] of large flares such as those that occurred on June 4th, 1991 and May 24th, 1990, it would be possible to record the tracks of the high energy neutrons arriving within 1100 seconds after the flare. However, following this time, track information will not be obtainable. The cutoff neutron energy was calculated to be less than 50 MeV. For other flares such as those that occurred on Mar 22nd, 1991, Nov 24th, 2000 and Oct 28th, 2003, the sensor would be capable of recording the tracks of all arriving neutrons during the entire event.

### 4 Detection efficiency, Secondary proton spectrum and Estimated neutron flux

Here we discuss the neutron detection efficiency of this detector. Actually we have obtained the correction efficiency  $\epsilon$  by the Monte Carlo method, using the Geant4 program. In this calculation, the collisions between neutrons and carbon target are also taken into account of. The detection efficiency of neutrons for vertical incidence can be approximated by  $\epsilon = 3.45 \times E[\text{MeV}]^{-0.7118}$ . For the incidence with  $\theta = 10^\circ, 20^\circ$  and  $30^\circ$ , the coefficient (3.45) are replaced by 3.1, 2.9 and 2.6 respectively.

In the data analysis, another condition has been applied; the minimum energy deposited in the sensor exceeds 35 MeV. According to the Monte Carlo calculation, the detection efficiency  $\epsilon$  can be expressed by  $\epsilon = 1.15 \times (E[\text{MeV}] - 25) \times E[\text{MeV}]^{-1.8}$ . In fact the detection efficiency  $\epsilon$  could be approximated by a constant value 0.021 (almost 2%) in the energy range of incident neutrons  $E_n = 50\text{-}120$  MeV [12].

On the other hand, the Monte Carlo calculation tells us that the secondary proton spectrum with  $E_p > 35$  MeV induced by primary neutrons in the sensor can be well de-

scribed by a simple relation as  $(E_p/E_n)^{-1.5}$ . Then the secondary proton spectrum  $I_p$  presented in Figure 2 can be related with the primary spectrum of neutrons by the relation:  $I_p(>E_p) = A \int_{E_p}^{\infty} E_n^{-\gamma} \left( \int_{E_*}^{E_n} (E_p/E_n)^{-1.5} dE_p \right) dE_n = A E_p^{2-\gamma} / (2-\gamma) (2.5-\gamma)$  (Eq.A), where  $E_p$  should be higher than  $E_* = 35$  MeV.

The proton spectrum given in Figure 2 can be fit by a power law in the energy range of  $E_p = 45-85$  MeV with the differential power index of -1.75 or the integral power index -0.75 (Eq.B). In comparison with Eqs. A and B, the  $\gamma$  should be 2.75 ( $2-\gamma = -0.75$ ). This is an expected differential spectral index for primary neutrons from ISS.

In this paper we only provide the flux of observed protons. The differential spectrum of protons (the left side ordinate of Fig. 2) has been obtained by dividing the energy spectrum (presented in the right side of the ordinate) by the total observation time ( $T = 1.74 \times 10^7$  [sec]) and the effective acceptance of the detector ( $S\Omega = 50$  [cm<sup>2</sup>.str]). Here we have assumed the solid angle of the detector toward the ISS is 0.5 steradian. The data are presented in Figure 2 for regions excluding the SAA.

Finally we present a candidate of solar neutrons in Figure 3 detected by the NEM-FIB sensor on March 7, 2011. The right side was taken by the PMT located at the leading section of the ISS (x-z plane) and the left side image presents a photo taken from the down side of the sensor (y-z plane).

## 5 Possible detection of solar neutrons in association with the flare on March 7, 2011

We searched the signals of solar neutrons. In association with the solar flare on March 7, 2011 with the X-ray intensity of M3.7, we may see the signals of solar neutrons. The satellite was traveling in the shadow side of until 20:02UT. Therefore we searched proton tracks induced by neutrons coming from solar direction within 20 degrees after 20:02 UT. The satellite (ISS) passes over the polar regions every 45 minutes. So every 45 minutes an increase of the event rate is observed. The distribution of the event rate of each trajectory has a quite similar shape; about 30 events/min. over polar regions and 3 event/min. over the Equator. However the trigger rate between 19:50 and 20:20 UT of March 7, 2011 shows a different feature; an excess was observed in comparison with the other times. We regarded this enhancement of events produced by the additional signals, i.e., an arrival of neutrons from the Sun. In fact the event rate of (19:10-19:35 UT) coming from the *assumed direction of the Sun* was 14 events/30 min., while during the flare time of (19:55-20:20 UT), the number of events coming from *actual direction of the Sun* was 46. Statistical significance of this excess turns out to be  $9\sigma$ . Furthermore the *last* neutron event observed at 20:17:45 UT had an energy of 44 MeV. Neutrons with the energy of 44 MeV arrived on the Earth after 1300 sec than the light. Therefore the production time of this neutron was estimated as to be around 19:55 UT. In Figure 4, we present the

arrival time distribution of neutrons coming from the direction of the Sun.

*Acknowledgements* The authors acknowledge the crew of the space shuttle Endeavor who have successfully mounted the SEDA-NEM detector on the ISS Kibo exposed facility. We also thank to the member of the Tsukuba operation center of Kibo who are taking the SEDA-NEM data everyday.

## References

- [1] Minutes of the 12th Space Development Committee of the Ministry of Education, Science and Culture, chaired by Minister R. Chikaoka, Report Nos. 13-1 and 12-3. The committee met on 9 April, 1997.
- [2] T. Doke, Science Asahi, September issue of 1997.
- [3] For example in the occasion of one of the hardest solar flare event observed in September 29th 1989, an increase of events was observed after 30 minutes later than the peak time of X-rays by one of the channels of the GOES sensor (in the range of  $E_p = 640$  MeV-850 MeV). Solar Geophysical Data 543(1989) 156.
- [4] S. Shibata, JGR, 99 (1994) 6651.
- [5] R. Bütikofer, E.O. Flückiger, Y. Muraki, Y. Matsubara, T. Sako, H. Tsuchiya, and T. Sakai, Proceed. 27th ICRC (Hamburg), 8 (2001)3053.
- [6] Y. Muraki, H. Tsuchiya, K. Fujiki, S. Masuda, Y. Matsubara, H. Menjyo, T. Sako, K. Watanabe, M. Ohnishi, A. Shiomi, M. Takita, T. Yuda, Y. Katayose, N. Hotta, S. Ozawa, T. Sakurai, Y.H. Tan and J.L. Zhang, Astroparticle Physics, 28 (2007) 119.
- [7] L.X. González, F. Sánchez and J.F. Valdés-Galicia, NIMA613 (2010) 263.
- [8] K. Koga, T. Goka, H. Matsumoto and Y. Muraki, Proceeding of the 21st ECRS edited by Kudela, Kiraly and Wolfendale, (2008) 199-200.
- [9] K. Koga, T. Goka, H. Matsumoto, Y. Muraki, T. Obara and T. Yamamoto, Paper presented at the 31st ICRC (Lodz, Poland), paper number 831(2009) SH1.3.
- [10] I. Imaida, Y. Muraki, Y. Matsubara, K. Masuda, H. Tsuchiya, T. Hoshida, T. Sako, T. Koi, P.V. Ramana-murthy, T. Goka, H. Matsumoto, T. Omoto, A. Takase, K. Taguchi, I. Tanaka, M. Nakazawa, M. Fujii, T. Kohno and H. Ikeda, NIMA, 421 (1999) 99.
- [11] K. Watanabe, private communication.
- [12] For the n-p scattering process, the cross-section can be treated analytically. The correction factor is the product of a geometrical factor and a nuclear interaction factor. The correction factor is given by  $(1.0-0.8 \times (E_p/100 \text{ MeV})^{1.82}) (\text{geometrical}) \otimes (0.375 \times (E_n/100 \text{ MeV})^{-0.81}) (\text{interaction})$ . The n-p cross section was measured in an accelerator experiment and was determined to be 14 mb/sr in the forward region at 92 MeV.

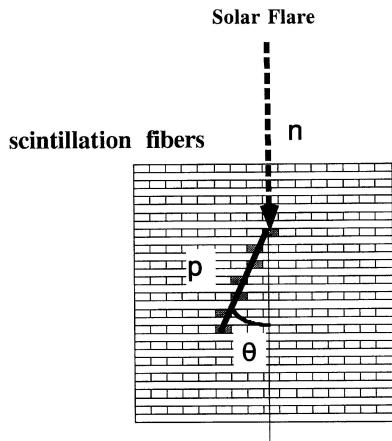


Figure 1: The schematic view of the FIB sensor of NEM. The FIB detectors consists of 16 layers of 16 sticks of the scintillation bars. Method of energy determination of neutrons by kinematics is schematically shown. Each layer is located alternatively along the x-direction and y-direction. The sensor is surrounded by the 6 plates of the scintillator and they are used for the anti-counter.

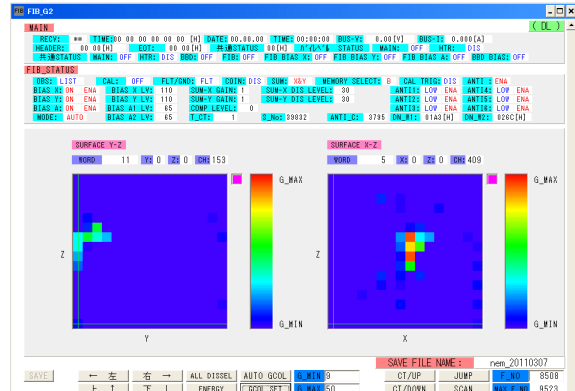


Figure 3: The second later arrival neutron detected at 20:14:57 UT by the NEM-FIB sensor. The energy of this neutron is estimated as to be 52 MeV. The direction of the Sun was down-side in the right panel (x-z plane). The right side photo was taken by the 256 channel multi-anode PMT from -x direction, while the left side screen represents the track seen from the -y direction by using another 256 channel multi-anode PMT (y-z plane). The direction of the Sun was located at the left side corner of the bottom side of y-z plane. The ISS proceeds toward -y direction. The color corresponds to the deposit energy in each scintillation bar.

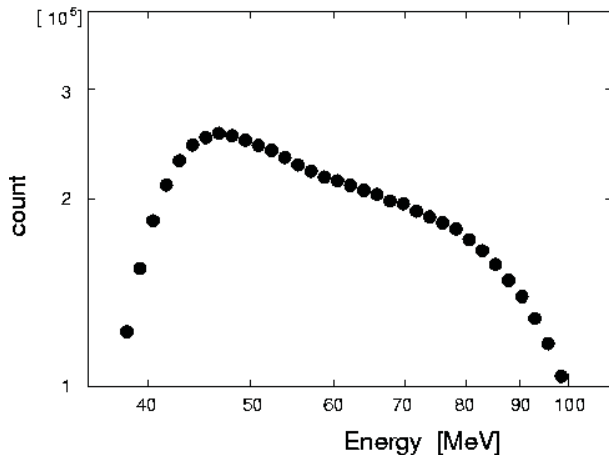


Figure 2: Secondary proton spectrum induced by neutrons observed by the NEM-FIB sensor. The data have been taken during the flight between January 1st 2010 and July 31st 2010. The differential intensity of protons is given in the right side of the ordinate, while the differential spectrum of secondary protons is given in the left side of the ordinate by the unit of  $particles/sec.sr.cm^2.MeV$

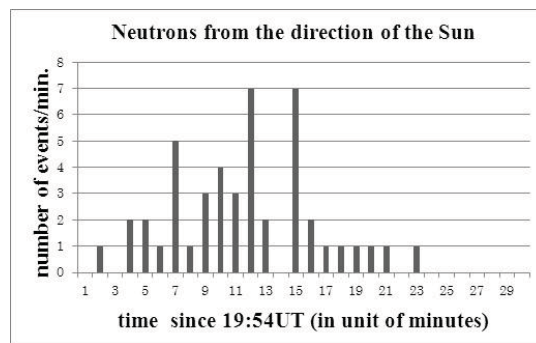


Figure 4: The arrival time distribution of neutrons that are consistent with solar neutrons, coming from the direction of the Sun with an opening angle less than 20 degrees. The events observed at 20:01 UT (7 + 19:54 UT) may correspond to neutrons elastically scattered with large angles at the top of the atmosphere and entered into the NEM-FIB detector, where the satellite was traveling still on the shadow side of the Earth. We need a detailed MC calculation for the interpretation of these events. The last event (23 + 19:54 UT) had an energy of 44 MeV.